Level structure and reflection asymmetry in ^{227}Th

C.F. Liang and P. Paris
Centre de Spectrométrie Nucléaire et de Spectrométrie de Masse, IN2P3, Centre National de la Recherche Scientifique, Bâtiment 104, 91405 Campus Orsay, France

R.K. Sheline
Chemistry and Physics Departments, Florida State University, Tallahassee, Florida 32306

D. Nosek and J. Kvasil
Department of Nuclear Physics, Charles University, V Holešovičkach 2, 18000 Prague 8, Czech Republic
(Received 1 November 1994)

The level structure of ^{227}Th has been studied using the electron capture decay of ^{227}Pa and the β^- decay of ^{227}Ac to give a total of 20 levels where only four were previously known. This level structure then makes possible a more complete interpretation of the recently studied ^{231}U alpha decay into ^{227}Th. The level structure can be interpreted using both strong coupling and intermediate coupling models in terms of $K = 1/2^{\pm}$, $K = 3/2^{\pm}$, and more tentative $K = 5/2^{\pm}$ parity doublet bands which implies that ^{227}Th has reflection asymmetry. Furthermore, the detailed interpretation of the level structure of ^{227}Th solves the long standing problem of the ground state spin parity of ^{227}Th which is shown to be $1/2^+$.

PACS number(s): 21.60.Ev, 23.40.−s, 27.90.+b

I. INTRODUCTION

Calculations [1] on the degree of intrinsic reflection asymmetry (IRA) possessed by ^{227}Th show that it is intermediate between that of ^{229}Th (which is known [1] to have coexistent configurations with both reflection symmetry and reflection asymmetry) and that of ^{225}Th [2] which has parity doublet bands as expected for normal IRA (see Fig. 1). The degree of IRA is given by the energy difference between mirror minima and the barrier which separates them. As shown in Fig. 1, this energy difference is ~1 MeV for ^{225}Th, while it is ~0.5 MeV for ^{227}Th and ~0.2 MeV for ^{229}Th. Thus it would be of interest to see experimentally whether ^{227}Th is IRA or whether, like ^{229}Th, there is experimental evidence for the coexistence of both reflection symmetric and reflection asymmetric configurations.

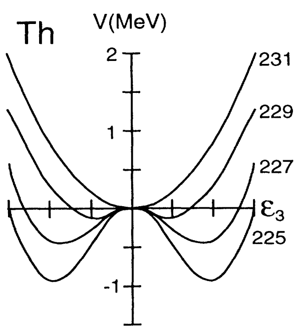

FIG. 1. Calculated potential energy diagrams [1] in octupole deformation coordinates for the odd-A Th isotopes from ^{225}Th through ^{231}Th. The larger barriers between the mirror minima correspond to more stable reflection asymmetric nuclei.

In addition, there is a long standing controversy [3] about the spin parity of the ^{227}Th ground state. The spin parity $3/2^+$ (suggested in earlier compilations [4,5]) was used in recent $\alpha - \gamma$ nuclear orientation experiments [6] to study the levels in ^{223}Ra. However, the most recent Nuclear Data Sheets compilation [3] as well as recent and earlier studies of the alpha decay of ^{227}Th suggest [7,8] $J^\pi = 1/2^+$ as the ^{227}Th ground state.

Actually, very little is known about the level structure of ^{227}Th. Up to the present time only four levels have been suggested—three as a result of the ^{227}Ac beta decay of Novikova *et al.* [9], and one additional one as a result of ^{231}U alpha decay [10].

Considering the paucity of information on the ^{227}Th levels, it is surprising that no one has studied the electron capture decay of ^{227}Pa into ^{227}Th. With a 15% electron capture branching ratio and a Q value of 1.026 MeV, the 38.3 m ^{227}Pa appears to be ideal for the study. We therefore propose to study the electron capture decay of ^{227}Pa and to re-study the β^- decay of ^{227}Ac in spite of its very limiting 43.7 keV Q value. We then use the level structure to attempt a further interpretation of the ^{231}U alpha decay studies [10].

II. EXPERIMENTAL METHODS AND RESULTS FROM THE ^{227}Pa ELECTRON CAPTURE DECAY

The ^{227}Pa was produced and isotope separated by a selective fluorination method developed at Orsay. A target

0556-2813/95/51(3)/1199(12)/$06.00

of ~10 g of an anhydrous powder of ThF_4 was bombarded by a 200 MeV and ~400 nA beam of protons in three separate experiments of durations varying from 32 to 48 h. It should be noted that the low beam intensity is necessary to keep the target as cool as possible (~ 500 °C) to sustain production of sufficient activity over a considerable period of time. CF_4 vapor was then passed over the target to facilitate fluorination. $^{227}PaF_4^+$ ions of mass 303 were separated using the ISOCELE separator with activity collected varying from 5×10^3 to 10^4 ions/s. The possible Th, Ac, Ra, and Fr activities are eliminated during the separation process because the corresponding ThF_3^+, AcF_2^+, RaF^+, and Fr^+ ions fall in totally different mass regions than the $^{227}PaF_4^+$ ions. Thus the selective fluorination method accomplishes both an isotope separation and a chemical separation simultaneously [11].

In the first experiment the ^{227}Pa activity was moved between two gamma ray detectors in a 180° close geometry. One of the gamma detectors had high resolution (~600 eV at 100 keV) but rather low efficiency for high energy gammas. It consisted of a 3 $cm^2 \times 5$ mm thick planar intrinsic Ge detector with a Be window. The other was a 20% efficient coaxial Ge detector. Singles gamma and $4K$-$4K$ gamma-gamma measurements were recorded simultaneously.

In the second experiment the tape transport system moved the collected ^{227}Pa activity into a magnetic selector where electrons were deflected by a uniform magnetic field into helical trajectories over a large energy range. After a 360° deflection they impinged onto a cooled 6 mm thick Si(Li) detector. A gamma detector and an alpha detector (not used in these experiments) were arranged in a plane with the Si(Li) detector. The gamma detector was of the coaxial Ge type, 20% efficient for gamma and x radiations. $4K$-$4K$ electron-gamma and gamma-gamma coincidence measurements were recorded.

The gamma spectra are shown in Figs. 2 and 3. Figure 2 is the gamma spectrum taken with the high resolution Ge detector in coincidence with the K x rays of Th observed in the high efficiency coaxial Ge detector. L and K x rays of Th are indicated and only the low energy region of ^{227}Th is shown. Figure 3 is the gamma spectrum taken with the high efficiency coaxial Ge detector in coincidence with the K x rays of Th observed in the high resolution Ge detector. The coaxial detector cuts off at low energy so that the L x rays are not observed. However, gamma rays of ^{227}Th are observed to much higher energies along with the Th K x rays.

The internal conversion electron spectra coincident with 151.1 and 56.4 keV gammas are shown in Figs. 4(a) and (b), respectively. The L, M, and N branchings are shown for the lower energy electron spectra, and K and L for the higher.

Table I lists the energies, intensities, and multipolarities of all the gamma rays observed following the electron capture decay of ^{227}Pa. The assignment of the transitions in the level scheme is also given in Table I. It should be noted that more than 90% of the gamma intensity has been assigned.

The level scheme for ^{227}Th as deduced from the decay of ^{227}Pa is given in Fig. 5. Three levels are shown dashed. Although their placement as shown is very probable, especially when model considerations are taken into account, they are based on energy fits rather than coincidence relationships. Dashed transitions are those which are used a second time and not based on coincidence relationships. The 90.0 keV transition corresponds to the energy of one of the K x rays of Th. The 9.3, 15.0, and 24.3 keV transitions marked only with the $E2$, $M1$, and $M1$ multipolarities in the lowest energy region of the level scheme result from the earlier ^{227}Ac decay study [9] and lead to the spins of $1/2^+$, $5/2^+$, and $3/2^+$ for the ground state, 9.3 keV state and 24.3 keV state as previously suggested [3,10,12]. The only other previously observed state at 77.7 keV was very tentatively assigned spin $5/2^+$ [10]. With $M1$ depopulating transitions to both the $5/2^+$ and $3/2^+$ states at 9.3 and 24.3 keV, either $3/2^+$ or $5/2^+$ are possible assignments. We prefer $J^\pi = 3/2^+$ for the 77.7 keV state because a $3/2^+$ member of the $K = 1/2^+$ band is expected in this vicinity.

The other low lying state at 37.9 keV decays by two $E1$ transitions to the $5/2^+$ and $1/2^+$ states at 9.2 keV and 0 keV. Its J^π is therefore unambiguously determined as $3/2^-$.

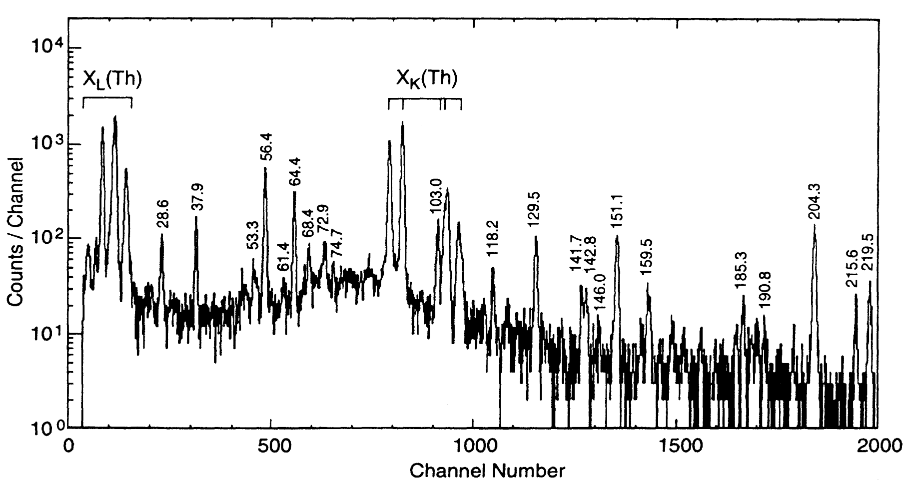

FIG. 2. Gamma spectra observed following the electron capture decay of ^{227}Pa taken with a high resolution planar Ge detector in coincidence with the K x rays of Th. Only the lower region of the gamma rays of ^{227}Th is shown.

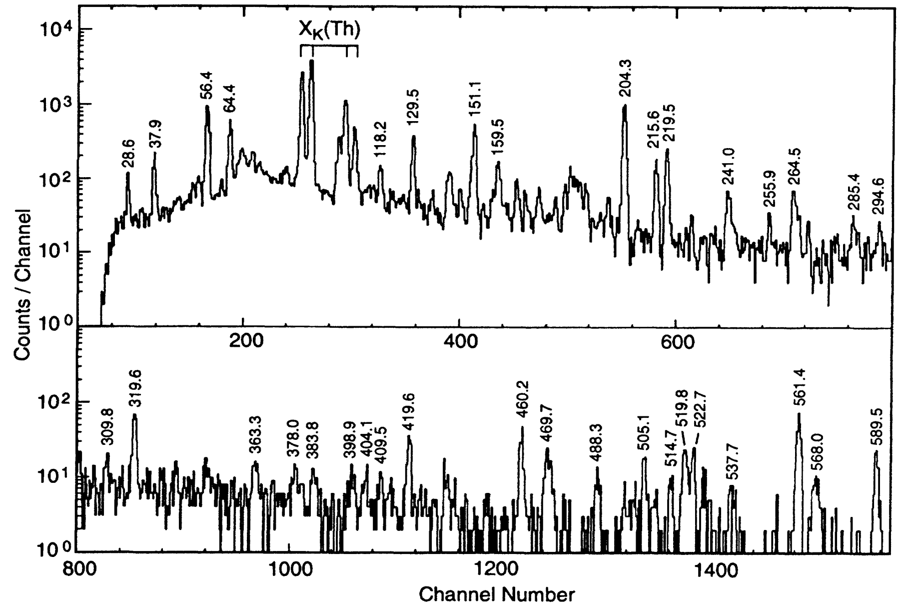

FIG. 3. Gamma ray spectra observed following the electron capture decay of ^{227}Pa taken with a high efficiency coaxial Ge detector in coincidence with the K x rays of Th. ^{227}Th gamma energies are given in keV and the region of the Th K x rays is indicated.

We have used the calculations of Leander and Chen [12] as the basis for many of the higher spin assignments which cannot be determined unambiguously from this experiment. In this interpretation the ground state $1/2^+$ and the $3/2^-$ 37.9 keV state are the bandheads of $K = 1/2^{\pm}$ bands, while the $3/2^+$ 24.3 keV state is the bandhead of a $K = 3/2^+$ band. One expects then a $K = 3/2^-$ parity doublet partner to the $K = 3/2^+$band. A level at 142.0 keV depopulates via a 64.4 keV $E1$ transition to the $3/2^+$ 77.7 keV state. The rest of the band structure suggests that this is the expected $K = 3/2^-$ bandhead. Three to five members of each of these four bands are observed experimentally and are consistent with the expected energies and spins. Bandheads at 448.0 and 547.0 keV are consistent with spin-parity assignments of $5/2^-$ and $5/2^+$. However, while the levels are quite definite the spins, parities, and band structures are not as well established as most of the low energy structure. The two highest energy states, observed experimentally at 688.7 and 698.4, are not interpreted in this level scheme, although it is clear that the 688.7 keV state is associated in some way with the $K = 5/2^{\pm}$ bands in

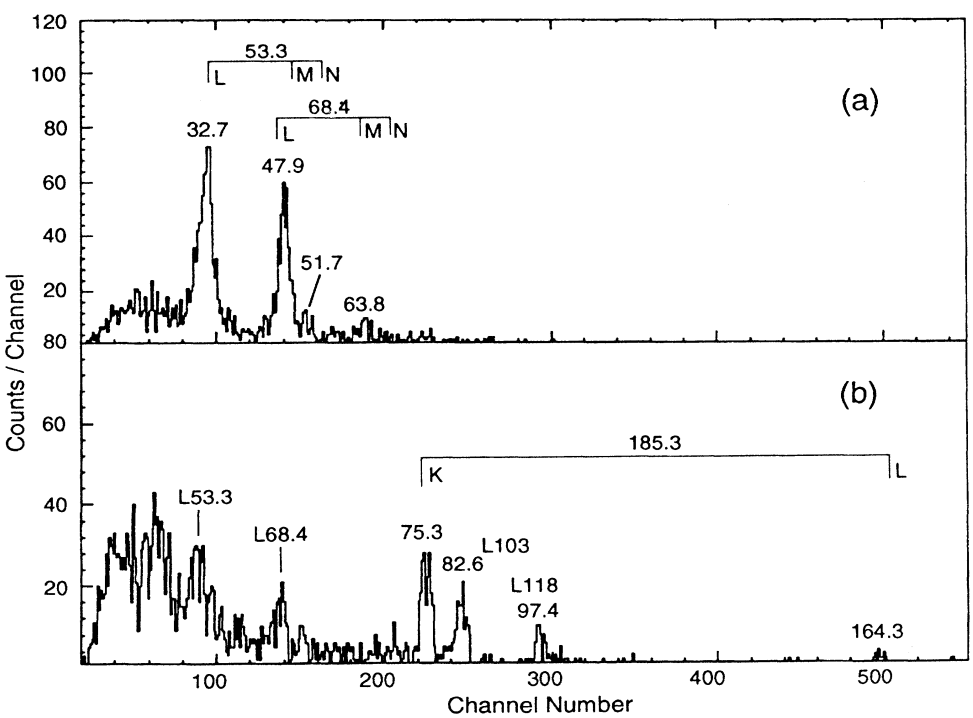

FIG. 4. (a) Electron conversion spectrum observed following the electron capture decay of ^{227}Pa in coincidence with the 151.1 keV gamma. L, M, and N branches of the conversion electron spectrum are indicated. (b) Electron conversion spectrum in coincidence with the 56.4 keV gamma.

TABLE I. Gamma ray energies and intensities of transitions in ^{227}Th observed in coincidences with X_KTh in the $^{227}\text{Pa} \overset{\text{c.e.}}{\rightarrow}$ ^{227}Th decay. Multipolarities when known, and assignments of transitions in the level scheme are also given.

$E_\gamma(\Delta E_\gamma)$	$I_\gamma(\Delta I_\gamma)$	Multipolarities	Levels Initial → Final
28.67 (0.05)	7.7 (1.0)	$E1$	37.9 → 9.3
37.89 (0.05)	9.0 (1.2)	$E1$	37.9 → 0
53.3 (0.2)	2.0 (1.0)	$M1(e^-)$	77.7 → 24.3
56.45 (0.05)	37.0 (3.0)	$E1$	183.7 → 127.3
61.4 (0.2)	~0.8		99.3 → 37.9
64.40 (0.05)	20.3 (3.0)	$E1$	142.0 → 77.7
67.2 (0.2)	~1.0		(67.2) → 0
68.4 (0.1)	2.9 (1.0)	$M1(e^-)$	77.7 → 9.3
72.7 (0.1)	6.0 (1.5)		(82.0) → 9.3
74.7 (0.2)	2.0 (1.0)		142.0 → 67.2
84.5 (0.3)	2.0 (1.0)		183.7 → 99.3
103.0 (0.1)	20.5 (2.5)	$M1(e^-)$	127.3 → 24.3
118.0[a] (0.2)	6.5 (1.5)	$M1(e^-)$	(142.0 → 24.3) 127.3 → 9.3
129.5[a] (0.1)	24 (3)	($E1$)	(228.7 → 99.3) 207.2 → 77.7
141.7 (0.2)	6.5 (1.5)		688.7 → 547.0
142.8 (0.2)	6.5 (1.5)		(224.9 → 82.0)
146.0 (0.3)	1.7 (1.0)		183.7 → 37.9
151.1 (0.1)	38.0 (4.0)	$E1$	228.7 → 77.7
157.7 (0.3)	2.0 (1.0)		
159.5 (0.2)	8.5 (2.0)		183.7 → 24.3
166.1 (0.3)	2.5 (1.5)		
168.9 (0.4)	2.0 (1.2)		
173.7 (0.4)	2.0 (1.2)		
185.3 (0.2)	12.0 (3.0)	$M1(e^-)$	688.7 → 503.4
190.8 (0.2)	8.0 (2.5)		228.7 → 37.9
204.3[a] (0.1)	100	$E1$	(688.7 → 448.0) 228.7 → 24.3
215.6 (0.2)	16.5 (3.0)	$M1(e^-)$	(224.9) → 9.3
219.5 (0.2)	28.0 (4.0)	$E1$	228.7 → 9.3
241.0 (0.3)	9.0 (3.0)		
255.8 (0.3)	3.5 (1.5)		
264.6 (0.2)	8.0 (2.0)		448.0 → 183.7
285.6 (0.5)	3.5 (1.5)		
294.6 (0.5)	3.5 (1.5)		547.0 → 252.1
300.0 (0.6)	3.3 (1.5)		
309.8 (10.5)	2.3 (1.0)		
319.6 (0.3)	9.5 (2.5)		503.4 → 183.7
363.3 (0.4)	3.5 (1.5)		547.0 → 183.7
370.0 (0.7)	~0.8		
378.0 (0.5)	2.0 (1.0)		
383.8 (0.5)	2.0 (1.0)		
398.9 (0.5)	2.0 (1.0)		
404.1 (0.5)	2.0 (1.0)		(503.4 → 99.3)
409.5 (0.5)	~1.0		(448.0 → 37.9)
419.6 (0.3)	6.5 (1.5)		547.0 → 127.3
432.7 (0.7)	2.0 (1.0)		
460.2 (0.4)	9.0 (2.5)		688.7 → 228.7
469.7 (0.4)	6.4 (1.5)		698.4 → 228.7
488.3 (0.4)	4.0 (1.5)		
505.1 (0.4)	4.5 (1.5)		688.7 → 183.7
514.7 (0.7)	2.5 (1.5)		698.4 → 183.7
519.8 (0.3)	7.0 (2.0)		
522.8 (0.3)	6.0 (2.0)		547.0 → 24.3
537.7 (0.7)	2.0 (1.0)		547.0 → 9.3
561.4 (0.3)	19.0 (3.0)		688.7 → 127.3
568.0 (0.5)	4.0 (2.0)		
589.5 (0.4)	7.0 (2.0)		688.7 → 99.3
609.2 (0.7)	2.0 (1.0)		

[a]Used twice in the level scheme.

view of the preferential strong population of these bands.

The position of the $1/2^-$ at 67.2 keV deserves special comment. A weak 74.7 keV transition has been shown to depopulate the 142.0 keV $3/2^-$ level. A weak 67.2 keV transition has also been observed. The sum of these two transition energies is 141.9 keV, well within error of 142.0 keV. This then defines a level at 67.2 keV with spin 1/2 or 3/2. Since we expect a $1/2^-$ band member of the $K = 1/2^-$ band is this vicinity (see Discussion), this is the model dependent assignment which is made.

Eighteen of the 20 levels in ^{227}Th observed in the decay of ^{227}Pa can be described in terms of six rotational bands or bandheads. However, it must be clearly noted that except for the four lowest energy levels, all of the spins and some of the parities assigned are model dependent. For that reason it is particularly fortunate that we have two independent decay studies with which to test the assignments. These decay studies are described in the next two sections.

III. LEVELS IN ^{227}Th OBSERVED IN THE β^- DECAY OF ^{227}Ac

As noted in the Introduction, Novikova *et al.* [9] studied the β^- decay of ^{227}Ac. They used an electron spectrometer and achieved remarkable results on the very low energy conversion electrons, successfully determining the multipolarities of the 9.3 keV transition as $E2$ and the 15.0 and 24.3 keV transitions as $M1$. This in turn led to the spin-parity assignments of the first three levels.

With a Q_β value of 44.8 keV, the gamma spectrum determination following β decay is not a very attractive project. Nonetheless, recognizing the existence of several low energy levels in the ^{227}Th level scheme, we decided to attempt it.

The ^{227}Ac activity used in these experiments was purchased from the Radiochemical Centre, Amersham, England. However, because of the age of the ^{227}Ac sample it was necessary to do a radiochemical purification to

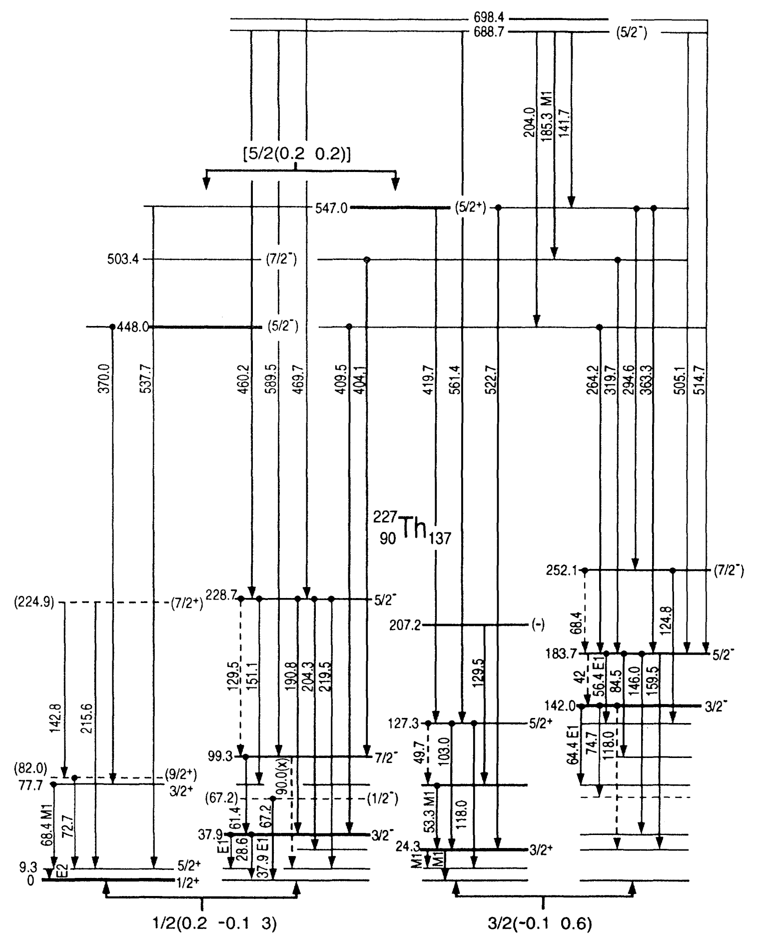

FIG. 5. The decay scheme of ^{227}Th as determined from the electron capture decay of ^{227}Pa. Transition energies are listed in keV, and multipolarities indicated where known. Alpha-gamma coincidences are indicated by a dot at the top of the gamma transition. Parity doublet bands and their configurations are also given. Except for the four lowest levels, all of the spins and some of the parities are model dependent. See the text for more details of the level scheme.

remove as many of the daughter contaminants (^{227}Th, ^{223}Ra, ^{219}Rn,...) as possible. The chemical purification was based on a solvent extraction between an α-thenoyltrifluoroacetone (TTA) phase in benzene and an aqueous phase buffered at pH 5.7. Under these conditions the ^{227}Ac and ^{227}Th are extracted into the TTA benzene phase while the other daughter products remain in the aqueous phase and are discarded. The ^{227}Ac was then returned to the aqueous phase by changing the pH to 1.0 while the ^{227}Th remained in the organic phase. The ^{227}Ac is evaporated to dryness and then evaporated in vacuum at 1800 °C onto a 30 μm Al foil.

The source was placed between a gamma and an electron detector in 180° close geometry. The gamma detector was a high resolution (600 eV at 100 keV) intrinsic Ge detector with a Be window. The electron detector which faced the evaporated side of the source was a Si(Li) wafer 700 mm^2 in area and 6 mm thick (with 2 keV resolution) placed inside a magnetic lens with axially increasing magnetic field. This lens has a large efficiency (2.3%) and large energy range [13].

In the first experiment gamma rays were measured with a freshly evaporated source. The result is shown in Fig. 6. Three (and possibly a fourth) low energy gamma rays are observed at energies of 24.5, 28.6, 37.9, and possibly 15.0 keV which can be assigned to ^{227}Th transitions. The 20.4 and 50.2 keV transitions result from the daughter ^{223}Ra.

In a second experiment the beta ray spectrum in coincidence with the 24.5 and 37.9 keV gamma transitions

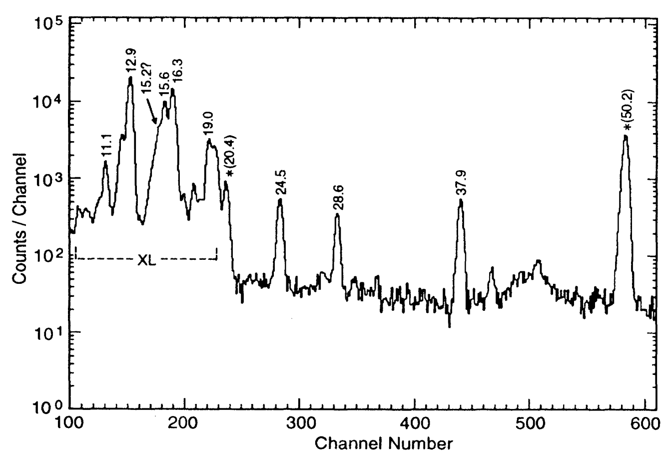

FIG. 6. Gamma rays following the β^- decay of ^{227}Ac immediately after purification from daughters. The levels indicated by an asterisk are gamma rays in the level scheme of ^{223}Ra. All levels below 19.0 keV except the possible 15.2 keV gamma ray are L x rays of Th.

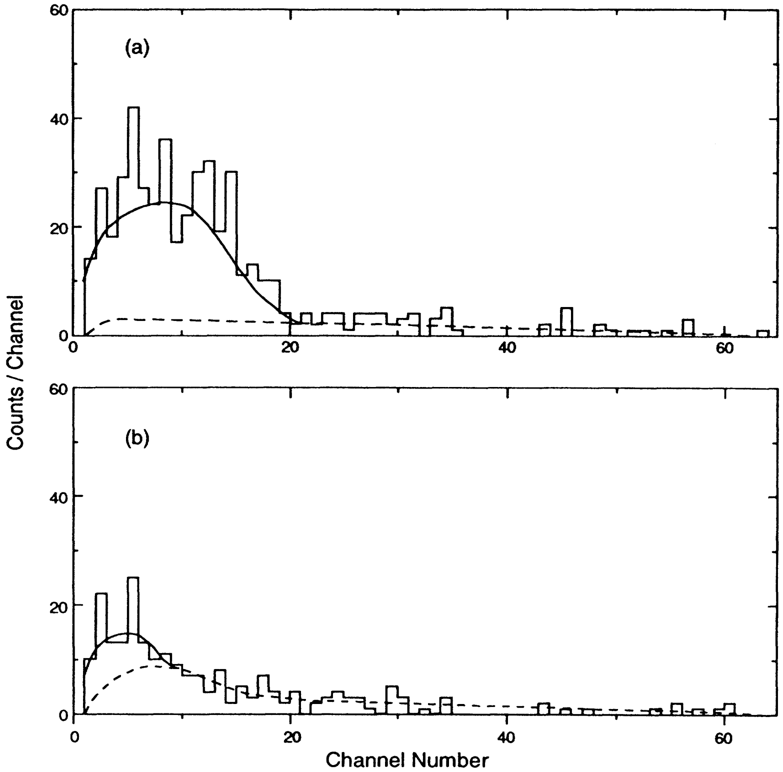

FIG. 7. (a) The β^- spectrum in coincidence with the 24.5 keV gamma in the β^- decay of ^{227}Ac. Background is shown dashed (end point energy=20.3 keV). (b) The β^- spectrum in coincidence with the 37.9 keV gamma in the β^- decay of ^{227}Ac. Background is shown dashed (end point energy=6.9 keV).

was observed with the Si(Li) detector. This is shown in Figs. 7(a) and (b), respectively. Since the Q_β is 44.8 keV for ^{227}Ac we expect end points of 44.8–24.5 keV and 44.8–37.9 keV or 20.3 and 6.9 keV for the spectra of Fig. 7(a) and Fig. 7(b), respectively. Although the statistics are not very good and the background high, particularly for the β^- spectrum feeding the 37.9 keV level with only a 0.3% population, the qualitative results are approximately what is expected.

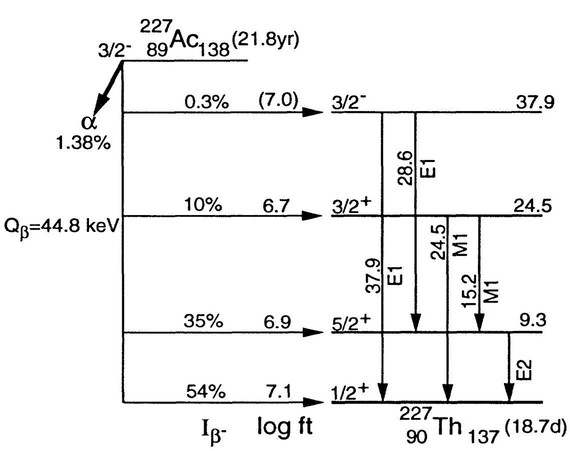

FIG. 8. The level scheme of ^{227}Th as observed following the β^- decay of ^{227}Ac. The $\log ft$ for populating the 37.9 keV level is shown in parentheses because of the uncertainty introduced by the long extrapolation of the $\log ft$ value from 10 keV to 6.9 keV [27].

Referring now to the spectrum of Fig. 5 one sees that the ground state and the lowest three excited levels of ^{227}Th have been populated in the β^- decay of ^{227}Ac. This is shown in the level scheme for the β^- decay of ^{227}Ac (Fig. 8).

IV. LEVELS IN ^{227}Th OBSERVED IN THE ALPHA DECAY OF ^{231}U

Recently [10] the alpha decay of ^{231}U was studied to deduce levels in ^{227}Th. The fine structure in the alpha decay was observed and three levels in ^{227}Th were shown to be populated. However, two additional gamma rays were observed following alpha decay which could not be fitted into the simple four-level decay scheme produced in this research. In view of the more complete level scheme of ^{227}Th now available, it seems appropriate to see if these two gamma rays with energies of 64.3 and 67.0 keV fit into the presently known level scheme and how that changes our view of the alpha decay of ^{231}U.

The level scheme of ^{227}Th (Fig. 5) shows that within the experimental error the 64.3 keV transition corresponds to the 64.4 keV $E1$ transition depopulating the 142.0 keV $3/2^-$ state to the 77.7 keV $3/2^+$ state. Furthermore, the 67.0 keV transition fits within the experimental error with the 67.2 keV transition depopulating the $1/2^-$ 67.2 keV state to the $1/2^+$ ground state.

We know from the ^{227}Pa $\rightarrow$ ^{227}Th studies that the 74.7 keV gamma transition depopulating the 142.0 keV level to the 67.0 keV state (not seen in the ^{231}U alpha decay) is only about 1/10th as strong as the 64.3 keV gamma depopulating the 142.0 keV state (see Table I and Fig. 5). However, when internal conversion coefficients are included (assuming $M1$ multipolarity) the depopulation via the 74.7 keV transition is ~0.6 that of the 64.3 keV transition. This allows us to determine the approximate alpha intensity populating the 142.0 keV state as ~0.8%. Using the intensity of the 67.0 keV transition and subtracting the intensity of the 74.7 keV transition we get a residual alpha-populating intensity of 0.2% populating the 67.0 keV state. However even this is an upper limit since we know nothing about the intensity of the expected 77.7 keV to 67.0 keV transition.

It is of considerable interest that the alpha decay of ^{231}U places the 67.2 keV transition in the lower part of the ^{227}Th level scheme. It buttresses the somewhat shaky assignment of the $1/2^-$ level at 67.2 keV. The resultant ^{231}U alpha decay scheme is shown in Fig. 9.

The fact that the ^{227}Ac β^- decay and the ^{231}U alpha decay confirm the ^{227}Th level scheme observed following ^{227}Pa electron capture decay gives us confidence in the level scheme in spite of the fact that many of the spins are model dependent. We will proceed then to the Discussion section to further interpret the level scheme of ^{227}Th and to understand its implications in a broader sense.

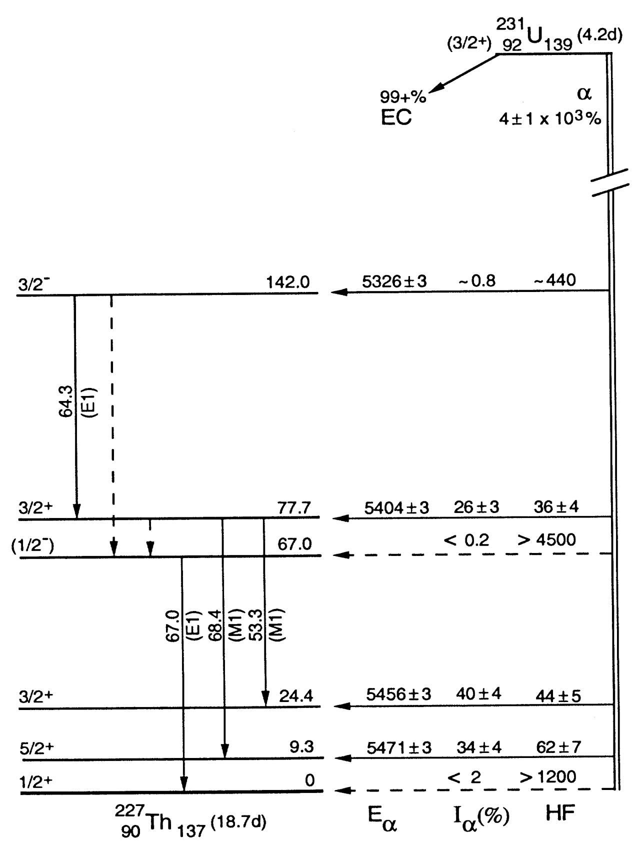

FIG. 9. The level scheme of ^{227}Th as observed following the alpha decay of ^{231}U. The spins of the 67.0, 77.7, and 142.0 keV levels are model dependent. This is an extension of the level scheme in Ref. [10].

V. DISCUSSION

The presence of parity doublet bands (bands with the same spin but opposite parity, close together in energy and connected by strong $E1$ transitions) in ^{227}Th (Fig. 5) is the single dominating feature of the level scheme. The existence of these parity doublets, together with the presence of decoupling parameters of the $K = 1/2^{\pm}$ parity doublet bands which are similar in magnitude but opposite in sign, are telltale signs of reflection asymmetry in ^{227}Th. The two alternative theoretical techniques of treating reflection asymmetry are the intermediate coupling and strong coupling models.

A. Intermediate coupling model and mixing of bands

Even a cursory view of the level scheme of ^{227}Th of Fig. 5 indicates that there is considerable Coriolis coupling between the $K = 1/2^{\pm}$ and $K = 3/2^{\pm}$ parity doublet bands. This is borne out by the anomalous energy spacing of the $3/2^+$, $5/2^+$, $7/2^+$ $K = 3/2^+$ band, and to a lesser extent, in a similar way with the $K = 3/2^-$ band. Furthermore the anomalous structure in these $K = 3/2^{\pm}$ bands is clearly due to the energy shifts expected from the interactions with the $K = 1/2^{\pm}$ bands. For example, it is difficult to say to which bands the $3/2^+$ states at 24.3 and 77.7 keV belong. In fact they are obviously so mixed that they both have considerable $K = 1/2^+$ and $K = 3/2^+$ character.

However, to give some quantitative idea of the degree of mixing we have calculated the values of the inverse moment of inertia, $\hbar^2/2\Im$, the decoupling parameter, a, and the bandhead energy, E_0, using three band energies from both $K = 1/2^+$ and $1/2^-$ bands. We then used these parameters to calculate other band members for comparison with experiment.

Specifically, we used the equation $E_I = \hbar^2/2\Im[I(I+1)+a(-1)^{I+1/2}(I+1/2)]+E_0$ without Coriolis coupling. Then for the $1/2^+$, $5/2^+$, and $3/2^+$ states at 0, 9.3, and 77.7 keV in ^{227}Th, we calculate $\hbar^2/2\Im = 4.58$ keV, $a = 4.66$, and E_0=17.9 keV. Using these values of the band constants we calculate the energy of the $7/2^+$ band member as 175.3 keV compared with the observed energy of 224.9 keV, and the $9/2^+$ band member as 24.6 keV compared with the experimental energy of 82.0 keV. In a similar way we used the 37.9, 99.3, and 228.7 keV $3/2^-$, $7/2^-$, and $5/2^-$ states and calculated $\hbar^2/2\Im$=9.84 keV, $a = -2.88$, and E_0=57.7 keV for the $K = 1/2^-$ band. In turn we then calculated the energy of the $1/2^-$ band member as 93.35 compared with the experimental value of 67.2 keV.

It is thus quite obvious that Coriolis effects are extremely important in the $K = 1/2^{\pm}$ and $3/2^{\pm}$ bands of ^{227}Th. The intermediate coupling model is particularly useful in identifying the most prominent Nilsson configurations which can then be used in Coriolis coupling calculations.

The intermediate coupling model for treating reflection asymmetric nuclei utilizes an average nuclear field assumed to have the usual *reflection symmetric* form.

Coupling between octupole and quasiparticle degrees of freedom is treated as a long-range residual interaction. The multiphonon excitation model [14] and the quasiparticle phonon model [15] are microscopic variants of the intermediate coupling model.

We have chosen to use the standard axially symmetric rotor model [16] which includes Coriolis coupling. The intrinsic degrees of freedom are described by the quasiparticle phonon model of Soloviev [17]. We take into account only quadrupole-quadrupole and octupole-octupole isoscalar long-range residual interactions as well as the pairing residual interaction. For the detailed method see Ref. [18].

In the first step of the analysis, the eigenvalue problem of independent quasiparticles was solved. The Nilsson model with standard parametrization [19] was used. Deformation parameters of the Nilsson single particle average field were $\epsilon_2 = 0.15$ and $\epsilon_4 = -0.03$. The pairing gap parameters taken from Ref. [16] were $\delta_p = \delta_n = 0.850$ MeV for both protons and neutrons. In the second step, we calculated the intrinsic quasiparticle-phonon wave functions within the quasiparticle-phonon model. All parameters involved in the long-range residual interactions were determined by the energies of quadrupole and octupole vibrations of the neighboring even-even cores. Specifically, we used $\hbar\omega_2 = 0.800$ MeV and $\hbar\omega_3 = 0.300$ MeV. The last step of our analysis consists of Coriolis mixing calculations; only the lowest energy intrinsic states up to 600 keV were considered. We include three negative parity and six positive parity intrinsic bands with $K \leq 5/2$. The intrinsic energies, parameters of inertia, and decoupling parameters of experimentally observed rotational bands were treated as free parameters.

Results of our calculation on the intrinsic structure of individual states observed experimentally in ^{227}Th are summarized in Table II. The first column of this table contains the percentages of the various components which make up the majority of the wave function. These include both the quasiparticle and the quasiparticle-phonon components. We use the asymptotic quantum numbers of the Nilsson scheme as labels of individual quasiparticle states. The second column of this table contains the experimental bandhead energies. The theoretical bandhead energies obtained in Coriolis coupling calculations are presented in the third column, while the rightmost column gives the intrinsic energies prior to Coriolis coupling.

The important thing to note is that all of the experimentally observed intrinsic states in ^{227}Th possess quasiparticle-octupole components in their wave functions. This is caused by the strong octupole-octupole interaction between $g_{9/2}$ and $j_{15/2}$ neutron shells. If

TABLE II. Microscopic structure of the $K = 1/2^{\pm}$, $3/2^{\pm}$, and $5/2^{\pm}$ bands in ^{227}Th. All compositions $\geq 2\%$ are given.

Structure of intrinsic state		Exp. energy of lowest level in band (keV)	Theo. energy of lowest level in band (keV)	Theo. intrinsic energy of lowest level in band (keV)
$1/2^+[651]$	47%			
$1/2^+[640]$	11%			
$1/2^-[770] + Q_{30}^+$	19%	0.0($1/2^+$)	0.0	0.0
$3/2^-[761] - Q_{31}^+$	6%			
$1/2^-[770] - Q_{31}^+$	5%			
$1/2^-[521] + Q_{30}^+$	3%			
$1/2^-[770]$	80%			
$1/2^+[651] + Q_{30}^+$	10%	37.9($3/2^-$)	39.5	53
$3/2^+[641] - Q_{31}^+$	3%			
$1/2^+[651] - Q_{31}^+$	3%			
$3/2^+[642]$	54%			
$3/2^+[631]$	7%			
$3/2^-[761] + Q_{30}^+$	5%	24.3($3/2^+$)	39.2	42
$7/2^-[743] - Q_{32}^+$	3%			
$5/2^-[752] - Q_{31}^+$	3%			
$1/2^-[770] - Q_{32}^+$	2%			
$3/2^-[761]$	80%			
$3/2^+[642] + Q_{30}^+$	12%	142.0($3/2^-$)	180.3	116
$1/2^+[651] + Q_{31}^+$	3%			
$1/2^+[651] - Q_{32}^+$	2%			
$5/2^-[752]$	79%			
$5/2^+[632] + Q_{30}^+$	6%	448.0($5/2^-$)	456.0	462
$3/2^+[642] + Q_{31}^+$	5%			
$1/2^+[651] + Q_{32}^+$	2%			
$5/2^+[632]$	48%			
$5/2^-[752] + Q_{30}^+$	17%			
$7/2^-[743] - Q_{31}^+$	15%	547.0($5/2^+$)	547.2	574
$3/2^-[761] + Q_{31}^+$	7%			
$9/2^-[734] - Q_{32}^+$	4%			

both $g_{9/2}$ and $i_{13/2}$ positive parity neutron shells are important in the basis of intermediate coupling calculations, octupole correlations are spread out over the whole sets of single-particle states and octupole collectivity occurs in the $i_{13/2}$ neutron shell region which is expected to be filled in the ^{227}Th nucleus. This result is interpreted as considerable octupole softness of the nucleus. Further, strong octupole correlations are calculated between the $K = 1/2^{\pm}$ intrinsic states based on the $1/2^-[770]$ and $\{1/2^+[651], 1/2^+[640]\}$ orbits and between the $K = 3/2^{\pm}$ states where the odd neutron occupies $3/2^-[761]$ or $\{3/2^+[642], 3/2^+[631]\}$ orbits. These results provide the theoretical basis for parity doublet classifications for both $K = 1/2^{\pm}$ and $K = 3/2^{\pm}$ opposite parity partners. The structures of higher lying $K = 5/2^{\pm}$ states are built on the $5/2^-[752]$ and $5/2^+[632]$ orbits. The $K = 5/2^+$ state possesses an unusually large octupole component of its lower lying opposite parity partner.

It is especially interesting that when the shifts in energy levels due to Coriolis effects are taken out, the decoupling parameters are -2.68 for the $K = 1/2^-$ band and 2.97 for the $K = 1/2^+$ band. Thus the expectation of reflection asymmetric nuclei, that the decoupling parameters of $K = 1/2^{\pm}$ parity doublet bands will have similar absolute values, but opposite signs, is in unusually good agreement in ^{227}Th.

The comparison between the experimentally observed energy levels (left) and the theoretical calculations including Coriolis coupling (right) is presented in Fig. 10 for ^{227}Th. Corresponding levels are connected by dotted lines. While the agreement is quite good it should be noted that with six intrinsic energies, six moments of inertia, and two decoupling parameters as free parameters to calculate 18 levels, we must be cautious in assessing the agreement.

B. Reflection asymmetric band configurations

The coupling between low-lying octupole modes and the single-particle degrees is assumed to be very strong in the strong coupling model. This leads directly to an average nuclear field which has acquired stable reflection asymmetric deformation. In the intermediate coupling model, the average nuclear field is assumed to have the standard reflection symmetric form and the coupling between octupole and quasiparticle modes is treated as a residual interaction. In this section we have chosen to use the strong coupling model in treating ^{227}Th.

The calculated [1] octupole deformed neutron orbitals used in this interpretation of ^{227}Th are presented in Fig. 11. The calculation [1] employs the folded Yukawa potential [20,21]. Since the coupling between the odd neutron and the reflection asymmetric field is strong in this calculation, the resulting neutron basis states are parity mixed.

The octupole deformed Nilsson levels of Fig. 11 are plotted as a function of the quadrupole deformation ϵ for the constant value of octupole deformation, $\epsilon_3 = 0.08$. They are labeled by $\Omega(\hat{s}_z, \hat{\pi})$ and in the case of $K = 1/2$ orbitals by a third quantum number within parentheses, $(\pi\text{conj}| -\hat{j}_+ \mid R \text{ conj})$. Ω is the total angular momentum along the symmetry axis; $\hat{s}_z$ can be used with Ω to calculate magnetic moments. $\hat{\pi}$ varies from -1 to $+1$ and is zero for equal mixtures of positive and negative components; the last label (for $K = 1/2$ bands only) corresponds to the parity times the decoupling parameter, a. Neutron numbers are shown in circles at gaps. Shell model orbitals at $\epsilon = \epsilon_3 = 0$ are also given for some of the lower levels as indicated by the arrows.

If we now use the octupole deformed neutron orbitals of Fig. 11 to interpret the levels of ^{227}Th and assume a quadrupole deformation, ϵ, of $\sim$0.16, then the low-lying orbitals will lie between the 132 and 138 neutron number energy gaps. The 137th neutron of ^{227}Th should occupy the 1/2(0.2 $-$0.1 3) neutron orbital. Low-lying excited hole states are expected from the 3/2($-$0.1 0.6) and 5/2(0.2 0.2) orbitals. Experimentally we see $K = 1/2^{\pm}$, $3/2^{\pm}$, and $5/2^{\pm}$ parity doublet bands in this order. Furthermore, this is exactly the same sequence of parity doublet bands which are observed in the isotone ^{225}Ra [22–26].

However, it should be noted that the alpha decay from ^{229}Th which populates the levels in ^{225}Ra tends largely to populate only positive parity states. Indeed, the $K = 5/2^-$ band of the $5/2^{\pm}$ parity doublet band is not populated at all. We understand this because the ^{229}Th alpha-decaying parent ground state is largely reflection symmetric with Nilsson configuration $5/2^+[633]$ and at most only a small amount of 5/2($-$0.2 0.7) or 5/2(0.2 0.2). However, the ^{229}Th $5/2^+$ ground state alpha decays to the ^{225}Ra $5/2^+$ level at 236.7 keV with an alpha decay hindrance factor of 1.5. This implies that the $K = 5/2^+$ band in ^{225}Ra is very similar to the $K = 5/2^+$ ground state of ^{229}Th. If we assume a similar state of affairs in ^{227}Th, then the tentative $K = 5/2^{\pm}$ bands at 448 and 547 keV may have components of the reflection asymmetric orbitals 5/2(0.2 0.2) and 5/2($-$0.2 0.7) and also the reflection symmetric orbital 5/2[633]. Because of this the assigned orbital in Fig. 5 is shown in brackets. The higher-lying 688.7 keV state tentatively assigned $J^{\pi} = 5/2^-$ preferentially populates the $K = 5/2^{\pm}$ bands at 448 and 547 keV. This may imply the presence of both 5/2(0.2 0.2) and 5/2($-$0.2 0.7) reflection asymmetric orbitals and/or the $5/2^+[633]$ Nilsson orbital which are strongly interacting. The present experimental data are insufficient to sort out this complex situation.

In any case, the presence of three sets of parity doublets with $K = 1/2^{\pm}$, $3/2^{\pm}$, and $5/2^{\pm}$, in that order, has been observed. The lowest two of these parity doublets is well explained using the parity-mixed reflection asymmetric neutron orbitals of Fig. 11.

C. The controversy about the ground state spin of ^{227}Th

In earlier versions of the Nuclear Data Tables [5] and in the Table of Isotopes [4] the ground state spin parity of ^{227}Th was given as $3/2^+$. However, as pointed out by several authors [7,8,12] and tentatively accepted by

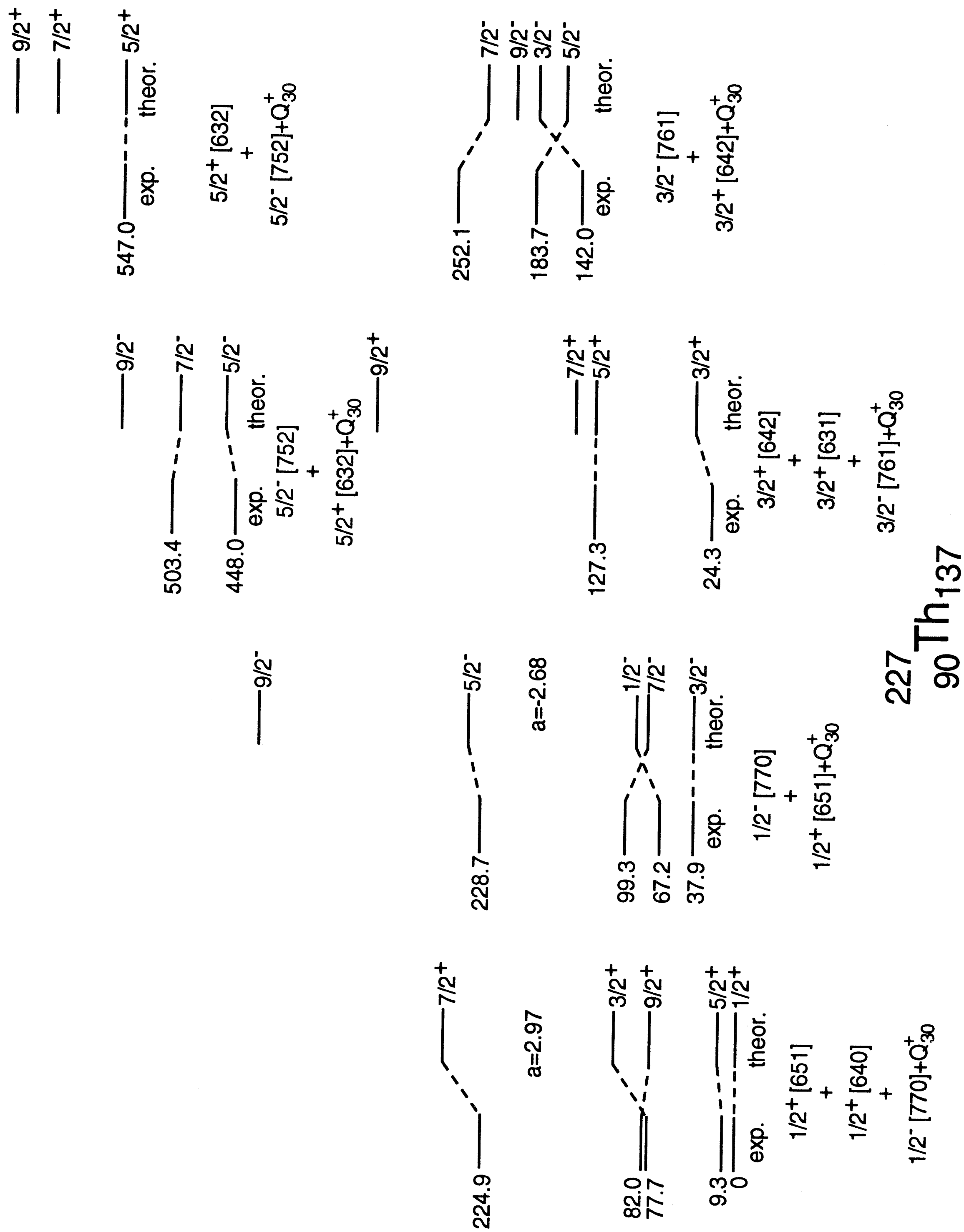

FIG. 10. Experimental and theoretical energies of the levels in ^{227}Th of the $1/2^{\pm}$, $3/2^{\pm}$ and $5/2^{\pm}$ parity doublet bands. The experimental levels, shown to the left, are connected by a dashed line with corresponding theoretical levels shown to the right. Except for the four lowest experimental levels, all of the spins and some of the parities are model dependent. Details of the calculations are given in the text.

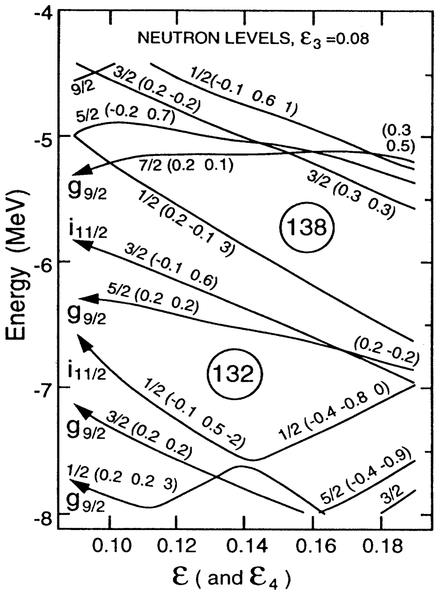

FIG. 11. Single neutron orbitals in an axially symmetric but reflection asymmetric folded Yukawa potential with $\epsilon_3 = 0.08$, plotted against the quadrupole deformation. For the labeling of the orbitals, see the text.

Nuclear Data Sheets [3], it seems much more probable that the ground state spin of ^{227}Th is $1/2^+$ in view of the very low alpha decay hindrance factors observed in the population of the $K = 1/2^\pm$ parity doublet bands in ^{223}Ra. However, fairly recently [6] the ground state spin of ^{227}Th has been assumed to be $3/2^+$ in extensive analysis of $\alpha - \gamma$ nuclear orientation experiments. If the ^{227}Th ground state spin is 1/2 then all of the nuclear orientation experiments would have given isotropic distributions of the gamma rays. In fact all of the reported distributions (some 36 in all) were anisotropic. While some of the anisotropies are only one or two times the experimental error, several of them are of the order of 10–20 times the experimental error.

Although a nonnuclear method of spin determination of the ^{227}Th ground state would still be desirable, in view of the extensive evaluation of the level structure of ^{227}Th provided by three different decays, we are confident that the spin parity is $1/2^+$.

VI. CONCLUSIONS

We have studied the level structure of ^{227}Th using the electron capture decay of ^{227}Pa and the β^- decay of ^{227}Ac. In addition we have reanalyzed the data from a recent experiment on the alpha decay of ^{231}U. By far the most extensive results are those from ^{227}Pa decay. The resulting level scheme from ^{227}Pa decay is confirmed by the ^{227}Ac and ^{231}U decays for all levels populated in these latter two decays.

While only the four lowest levels have experimentally determined spin parities, we are confident of the model dependent spin parities of the other 16 levels because of their internal consistencies and because of the cross-checks made possible by studying three different decays.

This experiment strongly suggests that the ground state spin parity of ^{227}Th is $1/2^+$.

The general nature of the level structure can be described in terms of three parity doublet bands with $K = 1/2^\pm$, $3/2^\pm$, and probably $5/2^\pm$. In view of these parity doublet bands and the fact that the decoupling parameters of $K = 1/2^+$ and $1/2^-$ bands have similar absolute values, but opposite signs, ^{227}Th has been shown to be reflection asymmetric.

The microscopic structure of the levels was calculated using an intermediate coupling model and the strongly mixed experimental levels compared with theoretical levels mixed through the Coriolis coupling.

Alternately, using the strong coupling model with octupole deformation $\epsilon_3 = 0.08$ and quadrupole deformation $\sim$0.16 we are able to interpret the $K = 1/2^\pm$ parity doublet bands as $1/2(0.2\ -0.1\ 3)$, the $K = 3/2^\pm$ parity doublet bands as $3/2(-0.1\ 0.6)$, and the tentative $K = 5/2^\pm$ parity doublet bands as $5/2(0.2\ 0.2)$.

ACKNOWLEDGMENTS

One of us (R.K.S.) would like to thank the National Science Foundation for support under Contract No. PHY92-07336 with Florida State University, and the CSNSM and the IPN at Orsay for their hospitality and joint support. Two of us (D.N. and J.K.) wish to thank the Granting Agency of the Czech Republic for support under Contract No. GAČR 202/94/0461.

[1] G.A. Leander and R.K. Sheline, Nucl. Phys. **A413**, 375 (1984).
[2] N. Schulz, Acta Phys. Pol. B **24**, 43 (1993).
[3] E. Browne, Nucl. Data Sheets **65**, 669 (1992).
[4] C.M. Lederer and V.S. Shirley, *Table of Isotopes*, 7th ed. (Wiley, New York, 1978).
[5] C. Maples, Nucl. Data Sheets **22**, 275 (1977).
[6] Ch. Briançon, S. Cwiok, S.A. Eid, V. Green, W.D. Hamilton, C.F. Liang, and R.J. Walen, J. Phys. G **16**, 1735 (1990).
[7] G.D. Jones, T.H. Hoare, P.A. Butler, and C.A. White, J. Phys. G **17**, 713 (1991).
[8] R.K. Sheline, G.A. Leander, and Y.S. Chen, Nucl. Phys. **A486**, 306 (1988).
[9] G.I. Novikova, E.A. Volkova, L.I. Goldin, D.M. Ziv, and E.F. Tretyakov, Zh. Eksp. Teor. Fiz. **37**, 928 (1959) [Sov. Phys. JETP **10**, 663 (1960)].
[10] C.F. Liang, R.K. Sheline, P. Paris, M. Hussonnois, J.F. Ledu, and D.B. Isabelle, Phys. Rev. C **49**, 2230 (1994).
[11] C.F. Liang, P. Paris, D. Bucurescu, S. Della Negru, J. Obert, and P.C. Putaux, Z. Phys. A **309**, 185 (1982); C.F. Liang, P. Paris, M.G. Porquet, J. Obert, and J.C. Putaux, *ibid.* **321**, 695 (1985).
[12] G.A. Leander and Y.S. Chen, Phys. C **37**, 2744 (1988).
[13] P. Paris *et al.*, Nucl. Instrum. Methods Phys. Res. Sect. A (to be published).

[14] R. Piepenbring, Z. Phys. A **323**, 341 (1986).
[15] V.G. Soloviev, Z. Phys. A **324**, 393 (1986).
[16] J. Kvasil, T.I. Kraciková, M. Finger, and B. Choriev, Czech J. Phys. B **31**, 1376 (1981); **33**, 626 (1983); **35**, 1084 (1985); **36**, 581 (1986).
[17] V.G. Soloviev, *Theory of Complex Nuclei* (Pergamon, Oxford, 1976).
[18] C.F. Liang, P. Paris, J. Kvasil, and R.K. Sheline, Phys. Rev. C **44**, 676 (1991).
[19] A.K. Jain, R.K. Sheline, P.C. Sood, and K. Jain, Rev. Mod. Phys. **62**, 393 (1990).
[20] M. Bolsterli, E.O. Fiset, J.R. Nix, and J.L. Norton, Phys. Rev. C **5**, 1050 (1972).
[21] P. Möller, S.G. Nilsson, and J.R. Nix, Nucl. Phys. **A229**, 292 (1974).
[22] K. Nybø, T.F. Thorsteinsen, G. Løvhøiden, E.R. Flynn, J.A. Cizewski, R.K. Sheline, D. Decman, D.G. Burke, G. Sletten, P. Hill, N. Kaffrell, W. Kurcewicz, and G. Nyman, Nucl. Phys. **A408**, 127 (1983).
[23] R.G. Helmer, M.A. Lee, C.O. Reich, and I. Ahmad, Nucl. Phys. **A474**, 77 (1987).
[24] G. Løvhøiden, T.F. Thorsteinsen, K. Nybø, and D.G. Burke, Nucl. Phys. **A452**, 30 (1986).
[25] R.K. Sheline, D. Decman, K. Nybø, T.F. Thorsteinsen, G. Løvhøiden, E.R. Flynn, J.A. Cizewski, D.G. Burke, G. Sletten, P. Hill, N. Kaffrell, W. Kurcewicz, G. Nyman, and G. Leander, Phys. Lett. **133B**, 13 (1983).
[26] ISOLDE Collaboration, E. Andersen, M.J.G. Borge, D.G. Burke, H. Geitz, P. Hill, N. Kaffrell, W. Kurcewicz, G. Løvhøiden, S. Mattson, R.A. Naumann, K. Nybø, G. Nyman, and T.F. Thorsteinsen, Nucl. Phys. **A491**, 290 (1989).
[27] N.B. Gove and M.J. Martin, Nucl. Data Tables **10**, 205 (1971).